Anomalous Excited-State Dynamics of Lucifer Yellow CH in Solvents of High Polarity: Evidence for an Intramolecular Proton Transfer

Debashis Panda, Padmaja P. Mishra, Saumyakanti Khatua, Apurba L. Koner, Raghavan B. Sunoj,* and Anindya Datta*

Department of Chemistry, Indian Institute of Technology Bombay, Powai, Mumbai 400 076, India

Received: November 1, 2005; In Final Form: February 27, 2006

The photophysics of the fluorescent probe Lucifer yellow CH has been investigated using fluorescence spectroscopic and computational techniques. The nonradiative rate is found to pass through a minimum in solvents of intermediate empirical polarity. This apparently anomalous behavior is rationalized by considering the possibility of predominance of different kinds of nonradiative processes, viz. intersystem crossing (ISC) and excited-state proton transfer (ESPT), in solvents of low and high empirical polarity, respectively. The feasibility of the proton transfer is examined by the structure determined by the density functional theory (DFT) calculations. The predicted energy levels based on the time-dependent density functional theory (TD-DFT) method in the gas phase identifies the energy gap between the S_1 and nearest triplet state to be close enough to facilitate ISC. Photophysical investigation in solvent mixtures and in deuterated solvents clearly indicates the predominance of the solvent-mediated intramolecular proton transfer in the excited state of the fluorophore in protic solvents.

1. Introduction

Lucifer yellow CH (LY CH) is the carbohydrazine derivative of a sulfonated N-substituted 1,8-naphthalimide, commonly used as a polar tracer.[1a] LY derivatives have been widely used in the study of biological systems as fluorescent labels and markers.[1,2] However, there have been very few efforts toward a systematic investigation on the fundamental photophysics of this class of compounds, until very recent times.[3] Our interest in LY CH stems from its potential use as a fluorescent probe for microenvironments. Recently, we have reported that LY CH binds to positively charged cetyltrimethylammonium bromide (CTAB) micelles and that binding is accompanied by a marked change in the nonradiative rates of the fluorophore.[3b] The absence of such an interaction in the anionic SDS and neutral Triton X 100 indicates that the binding of LY to micelles cannot take place by hydrophobic effect alone but requires some electrostatic assistance as well. From the results of a preliminary solvent variation study, we have proposed that polarity-dependent charge-transfer processes alone cannot determine the nonradiative rates in LY CH, especially in media of low empirical polarity.[3b] We were unable to determine the nature of the additional channels of radiationless depopulation of the excited state and had hypothesized that it could involve charge transfer as is observed in similar fluorophores[3a] and that the increase in k_{NR} upon binding with CTAB micelles could be due to a polarity effects. Subsequently, Fürstenberg and Vauthey have performed a fluorescence investigation of the excited-state processes of two derivatives of LY, namely, Lucifer yellow ethylenediamine (LYen) and Lucifer yellow biocytin (LYbtn).[3c] In this study the principal pathway identified for nonradiative decay of the S_1 state of LYen has been through intersystem crossing (ISC) in nonaqueous solvents, but excited-state proton transfer (ESPT) has been proposed to the major pathway in aqueous solutions. Such apparently anomalous behavior has been reported earlier for several other molecules and is generally obtained when some other solvent parameter like proticity or viscosity becomes more important than polarity for a particular nonradiative process.[4−6] Structural aspects can also affect the photophysics rather markedly, through a modification of the gaps between energy levels.[4,7,8] We have chosen LY CH because it is soluble in a greater number of solvents, as against the very limited solubility of LYen.[3b] Most importantly, it is soluble in alcohols, and so the photophysics can be studied in this class of protic solvents. With this advantage, LY CH has the potential of providing a better understanding of the photophysics of the molecules of the LY family. The possible differences in excited-state dynamics of LY CH from those of LYen are discussed later in this paper.

In the present work, we have studied the effect of different environmental parameters such as empirical polarity, viscosity, and proticity on the fluorescence properties of LY CH, as all these parameters can be important in governing the excited-state dynamics.[4−6] We have also performed density functional theory (DFT) calculations on the ground as well as the excited states of the molecule, to rationalize the experimental observations. As it is rather challenging to understand the photophysics of large molecules, it is imperative that experiments and theoretical calculations be performed in synergy in order to obtain a clear insight on the system.[4] Very often, an accurate knowledge of the structure is extremely helpful in the prediction of possible excited-state interactions. For example, an unexpected viscosity effect in calphostin C could be explained by considering the involvement of the bulky side chain present, once it was known from ab initio calculations that the terminal hydroxyl group of the side chain could be within hydrogen-bonding distance of carbonyl oxygen atoms in the fused ring system.[4b] Similarly, time-dependent density functional theory (TD-DFT) calculations were found to be of value in ruling out

* Corresponding authors. Phone: + 91 22 2576 7149. Fax: +91 22 2572 3480. E-mail: anindya@chem.iitb.ac.in (A.D.); sunoj@chem.iitb.ac.in (R.B.S.).

10.1021/jp056295q CCC: $33.50
Published on Web 04/08/2006

ESPT in coumarin 343[4c] and understanding the solvent dependence of pyrromethane dyes.[4d]

2. Experimental Section

Photophysical Studies. LY CH has been obtained from Molecular Probes and is used as received. Deionized water is distilled twice before being used as a solvent. Other solvents are of spectroscopic grade and are obtained from Spectrochem, Mumbai, India. These are distilled immediately prior to use. Deuterated solvents from Sigma-Aldrich have been used as received. The steady-state spectra are recorded on JASCO V570 spectrophotometer and Perkin-Elmer LS55 fluorimeter. $\lambda_{ex} =$ 400 nm for the fluorescence spectra. Fluorescence quantum yields (ϕ_f) are calculated after proper correction for changes in absorbance using TPP as the standard, ($\phi_f = 0.11$).[9a] Time-resolved fluorescence measurements have been performed at magic angle using a picosecond pulsed diode laser based TCSPC fluorescence spectrophotometer with $\lambda_{ex} = 406$ nm from IBH, U.K. ($\lambda_{em} = 530$ nm). The experiments have been performed at a resolution of 7 ps per channel. The fwhm of the instrument response function is 250 ps.[9b] Nonradiative rates are calculated from ϕ_f, and radiative lifetimes (τ_f) using the formula $k_{NR} = (1 - \phi_f)/\tau_f$.

Computational Details. The ground-state geometry of dianionic LY CH and LYen are optimized using the DFT method with the Becke3LYP functional,[10a,b] with the polarized 6-31G* basis set, as implemented in the Gaussian 98 suite of quantum chemical programs.[10c] The default options for the self-consistent field (SCF) convergence and threshold limits in the optimization by the DFT method are used. First, TD-DFT calculations are performed on the gas-phase optimized geometry of the ground state (S_0).[10d] The B3LYP functional in conjunction with a double-ζ quality basis set having diffuse functions, namely, the 6-31+G*, has been employed for the TD-DFT calculations. Vertical excitations are carefully analyzed by inspecting the corresponding Kohn−Sham orbital contours generated with the MOLDEN program.[10e] Next, long-range effects induced by solvent empirical polarity on the predicted photophysical properties are taken into account by means of dielectric continuum approach using Tomasi's polarizable continuum model (PCM).[10f] We have used the integral equation formalism[10g] within the PCM framework for the present study.

3. Results and Discussion

Nonradiative Rates in Neat Solvents. As has been reported earlier, there is a considerable Stokes shift of the emission spectra with respect to the absorption spectra in all solvents (Figure 1a). However, attempts to construct a Lippert plot do not yield satisfactory results. In solvents with low empirical polarity, LY CH exhibits unusually large values of Stokes shift.[3a] The fluorescence decays are also solvent dependent (Figure 1b). Earlier, we have observed that the plot of log k_{NR} rates with the empirical solvent polarity parameter $E_T(30)$ yields a straight line with a positive slope for the high-polarity solvents. This had prompted us to conclude that, in low-polarity solvents, the fluorophore exhibits unusual solvent behavior, akin to some of the coumarin dyes.[5b,c,6c] Further experiments have revealed that a weak, but distinct, linear variation can be obtained in solvents of low empirical polarity as well, but for these solvents, the line has a negative slope (Figure 2). The experiment would have been more comprehensive if we could have performed the measurements in more solvents, but unfortunately, the poor solubility of LY CH in many low-polarity solvents is the limiting factor here. Nevertheless, it is important to note that two distinct

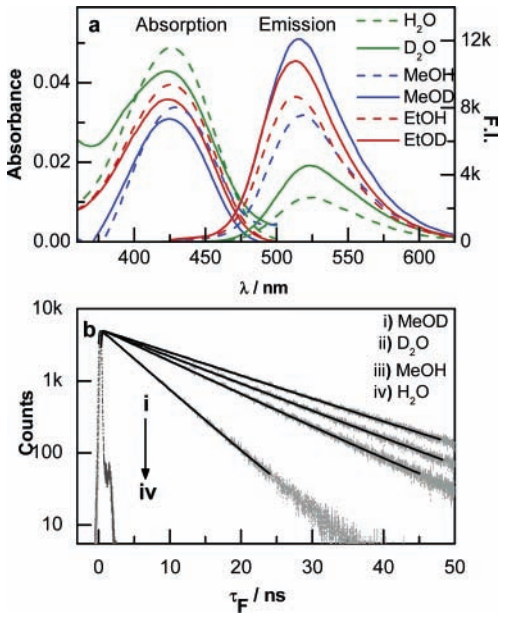

Figure 1. (a) Absorption and absorption-corrected emission spectra of LY CH. Solid lines: D_2O (green), MeOD (blue), and EtOD (red). Dashed lines: H_2O (green), MeOH (blue), and EtOH (red). $\lambda_{ex} = 406$ nm for the emission spectra. (b) Fluorescence decays of LY CH in (i) MeOD, (ii) D_2O, (iii) MeOH, and (iv) water. $\lambda_{ex} = 406$ nm. The solid lines denote the curves of best fit. The IRF is shown in dashed lines.

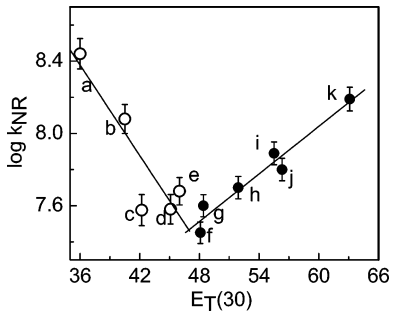

Figure 2. Plot of log k_{NR} with the $E_T(30)$ for (a) 1,4-dioxane, (b) pyridine, (c) acetone, (d) DMSO, (e) acetonitrile, (f) *n*-octanol, (g) propan-2-ol, (h) ethanol, (i) methanol, (j) ethylene glycol, and (k) water. The lines are the best fits to the data in the given range of $E_T(30)$.

regions with different types of dependence between nonradiative rates and empirical polarity are identified. The considerable deviation of the data points on either side of the lines is too large to be entirely due to errors in the experiment. It is more likely that they indicate different kinds of specific solvent effects. For example, there is a negative deviation for highly viscous solvents *n*-octanol and ethylene glycol and positive deviation for acetone which contains a C=O bond. Moreover, the question that arises now is whether the so-called unusual behavior is observed in the low-polarity or the high-polarity region, as there are weak linear correlations of opposite natures in the two regions. At this point, it is useful to recall that in the absence of excited-state reactions such as twisted intramolecular charge transfer (TICT), ESPT, photoisomerization, etc., log k_{NR} can have a direct as well as inverse variation with the $E_T(30)$ depending on the relative polarities of the ground and the excited states. In molecules with a more polar excited state than the ground state, there is a Stokes-shifted emission quantified by the well-known Lippert−Mataga equation.[11a] Moreover, in these kinds of molecules as the energy gap between the excited and the ground state decreases in polar solvents, there is an increase in the nonradiative rate with the empirical polarity parameter,

$E_T(30)$.[11b,c] However, if the ground state of the fluorophore is more polar than the excited state, then the energy gap increases on going to polar solvents, and the nonradiative rate can then decrease with an increase in polarity. Betaine dyes are most well-known examples that fall in this category.[11d] The increase in the energy gap between their ground and excited states forms the basis of the widely used $E_T(30)$ scale of polarity[11e] as observed in LYen.[3b] Such an effect can be ascribed to the dipole moments in the ground and excited states. Thus, it is essential to calculate the relative energies of the ground and excited states as a function of polarity in order to determine which of these two classes LY CH belongs to. In LYen, it has been proposed that the predominant nonradiative process in solvents of low polarity is ISC, whereas that in solvents with higher polarity and proticity is an excited-state intermolecular proton transfer. To get an idea of the energies of the different excited state, as well as to examine whether the molecular geometry can possibly permit additional nonradiatve process (like intramolecular proton transfer), we have performed DFT calculations, as is discussed in the next section.

TD-DFT Calculation. Full geometry optimization of the dianionic LY CH has been carried out at the B3LYP/6-31G* level of theory. The optimized structure is given in Figure 3, and key structural parameters are summarized in Table 1. Two intramolecular hydrogen bonds can be noticed, one involving the sulfonyl and other involving the carbonyl groups as hydrogen bond acceptors. This structural feature assumes additional relevance in the context of a likely intramolecular proton transfer in the excited state, as is elaborated later. Moreover, to compare the structural as well as energy level diagrams between LY CH and LYen, the geometry of latter has also been optimized at that same level of theory (i.e., B3LYP/6-31G*). The optimized structure of LYen shows no intramolecular hydrogen bond involving the carbonyl group as a hydrogen bond acceptor (Figure 3). Thus, the possibility of an intramolecular proton transfer in LYen is ruled out at this point. The computed dipole moments for these compounds are as high as 13.63 and 10.73 D for LYCH and LYen, respectively, reminiscent of dianionic species.

Next, we have decided to look at the vertical excitations using the TD-DFT with the B3LYP functional on the optimized geometry of singlet ground state of LY CH. At the first place, inspection of the Kohn−Sham orbital contours for the frontier MOs has been done, which reveals that the HOMO, LUMO, and LUMO + 2 are mainly π-type orbitals delocalized over the naphthyl as well as carbonyl units. These orbitals along with corresponding energies are depicted in Figure 4. The highest intensity transition is found to be of a $\pi-\pi^*$ type, predominantly between the HOMO and LUMO. The predicted wavenumber (24116 cm^{-1}) (Table 2) for the highest intensity transition in the lower energy region is found to be in fairly good agreement with the most intense experimental absorption maximum measured in aqueous medium.[10h]

Another interesting observation emerging from the computed results pertains to the energetic separation between the low-lying singlet and triplet states. Excitation energies for three lowest singlet and triplet states are schematically represented in Figure 5. It is apparent that the energy gap between the S_1 and nearest triplet state T_2 is rather small in the gas phase, a situation that could ensue a facile ISC. While this prediction based on the gas-phase calculations is important enough, the effect of various solvents on the excited-state energies can be crucial to the observed photophysics. Thus, we have considered using the PCM with the integral equation formalism (IEFPCM).[10e]

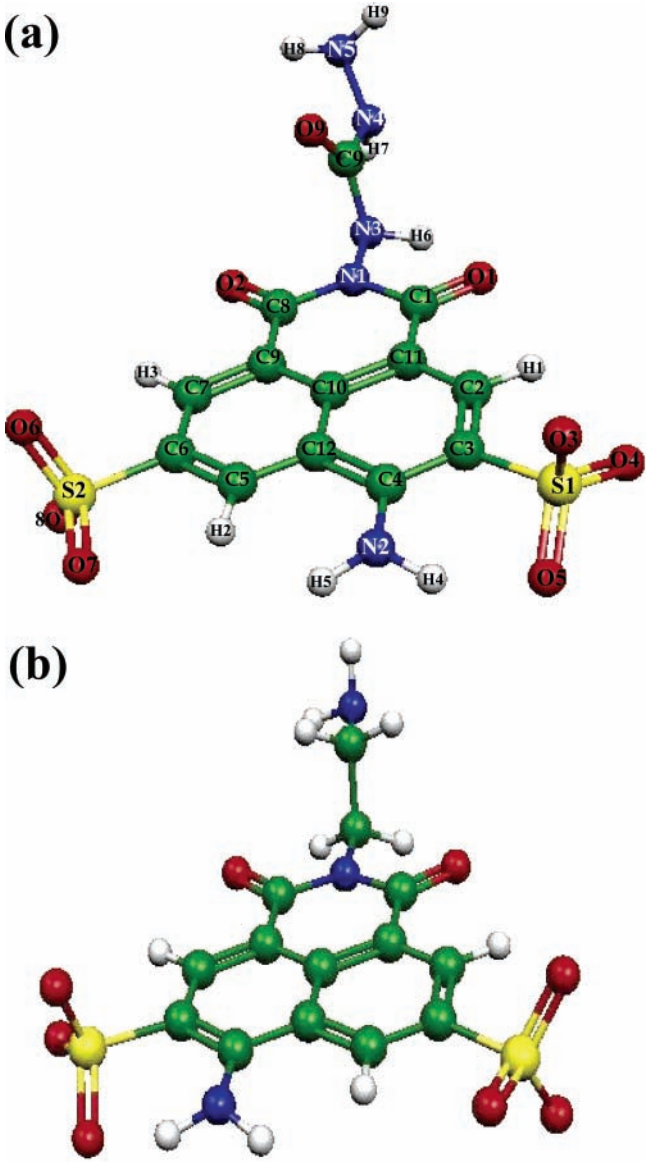

Figure 3. B3LYP/6-31G* optimized geometries: (a) LY CH and (b) LYen.

The computed data reveals that the highest intensity transition in the lower energy region, characterized as $\pi-\pi^*$, remains nearly the same, irrespective of the nature of the solvent. Interestingly, the computed absorptions at different wavelength regions, as indicated by the vertical lines, are by and large quite consistent with experimentally obtained spectra (Figure 6). The absorption is found to undergo a modest blue shift in polar solvents.[10h] In solvents such as acetone and water the second triplet excited state (T_2) is found to be relatively destabilized compared to that of the gas phase. Thus, the nearest accessible triplet (S_1, T_1) that can facilitate ISC is now at a larger separation than that in the gas phase (S_1, T_2). Hence, we propose that even though ISC may be the predominant nonradiative process in the gas phase and in solvents of low polarity, its efficiency is expected to diminish as the polarity of the medium increases. This could explain the negative slope in the plot of log k_{NR} against $E_T(30)$ in the low-polarity region. In high-polarity solvents such as acetone and water, where the nonradiative rates are expected to be same in both cases if an ISC from S_1 to T_1 is the principal pathway in these solvents, the calculated S1−T1 energy gap is very large. This is quite surprising for a transition with a large variation of electric dipole moment

TABLE 1: B3LYP/6-31G* Optimized Geometrical Parameters of [LY CH]$^{2-}$

B3LYP/6-31G*			
bond lengths		bond angles	
C1−O1 (C8−O2)	1.237 (1.223)	N1−C1−C11 (N1−C8−C9)	115.5 (114.3)
C1−C11 (C8−C9)	1.447 (1.476)	C9−C10−C11 (C1−N1−C8)	121.4 (127.6)
C1−N1 (C8−N1)	1.420 (1.412)	C11−C2−C3 (C9−C7−C6)	122.2 (120.4)
C2−C11 (C7−C9)	1.399 (1.389)	C2−C3−C4 (C5−C6−C7)	119.9 (119.4)
C2−C3 (C6−C7)	1.389 (1.404)	C3−C4−C12 (C6−C5−C12)	119.3 (122.0)
C3−C4 (C5−C6)	1.417 (1.383)	C2−C3−S1 (C7−C6−S2)	118.3 (120.3)
C4−C12 (C5−C12)	1.450 (1.416)	N2−C4−C12 (N2−C4−C3)	120.7 (120.0)
C3−S1 (C6−S2)	1.829 (1.826)	C4−N2−H4 (C4−N2−H5)	118.9 (114.7)
N3−C13 (C13−N4)	1.401 (1.403)	N1−N3−C13 (N3−C13−O9)	116.3 (126.9)
N2−H4 (N3−H6)	1.008 (1.022)		
S1−O3 (S1−O5)	1.484 (1.505)		
S2−O6 (S2−O8)	1.487 (1.490)		
C9−C10 (C10−C11)	1.425 (1.423)		
C10−C12	1.427		
O1−H6	2.084		
O4−H5	1.836		
dihedral angles			
N1−C1−C11−C10 (N1−C8−C9−C10)		2.5 (−0.34)	
N1−C1−C11−C2 (N1−C8−C9−C7)		178.6 (−178.1)	
C1−N1−C8−C9 (C1−C11−C10−C9)		7.2 (0.5)	
C9−C10−C12−C5 (C9−C7−C6−C5)		−0.7 (0.5)	
C11−C10−C12−C4 (C4−C3−C2−C11)		0 (0.9)	
C2−C3−C4−C12 (C2−C11−C10−C12)		−1.0 (0)	
C7−C6−C5−C12 (C7−C9−C10−C12)		−0.2 (0)	
C11−C1−N1−N3 (C9−C8−N1−N3)		175 (−175.2)	
N1−N3−C13−O9 (O9−C13−N4−N5)		−6.6 (−9.5)	
dipole moment		13.63	

making LY a good polarity probe. However, from Figure 2, it is apparent that there is a steady increase in log k_{NR} on going from acetone to water. This indicates that some other nonradiative pathway becomes predominant in solvents with higher polarity. Thus, the theoretical prediction in case of LY CH is in agreement with the experimental observation with LYen in less polar and aprotic solvents,[3b] and we assign the principal nonradiative process in low empirical polarity to ISC. Consequently, in this report, the energy level diagram of LYen is also presented.[10h] The relative ordering of the levels turns out to be very similar to that in LY CH. It has been reported earlier that ISC is the predominant nonradiative channel for LYen in low-polarity solvents. The present calculations are in agreement with this observation. Moreover, we can extrapolate this agreement, to expect that ISC is also the major nonradiative pathway for LY CH in solvents of low polarity. As has been mentioned earlier, an intermolecular proton transfer has been proposed to be the principal nonradiative channel in water for LYen. The high-polarity solvents that we have used are protic solvents such as alcohols. As the nonradiative rate increases in these solvents, the possibility of occurrence of an intermolecular or intramolecular proton transfer in the excited state is fairly high. As discussed earlier one can expect from the molecular geometry (Figure 3) that such an intramolecular proton transfer would involve the N_3, H_6, and O_1 atoms. The rate of such a proton transfer is expected to be viscosity dependent, as the NH group is part of a five-membered chain and proton transfer in the excited state involving the motion of such chains is often dependent on the viscosity of the medium.[4b] So, we have performed a preliminary study on the fluorescence properties of LY CH in solvent mixtures to examine the effect of viscosity, if any, on the nonradiative rates.

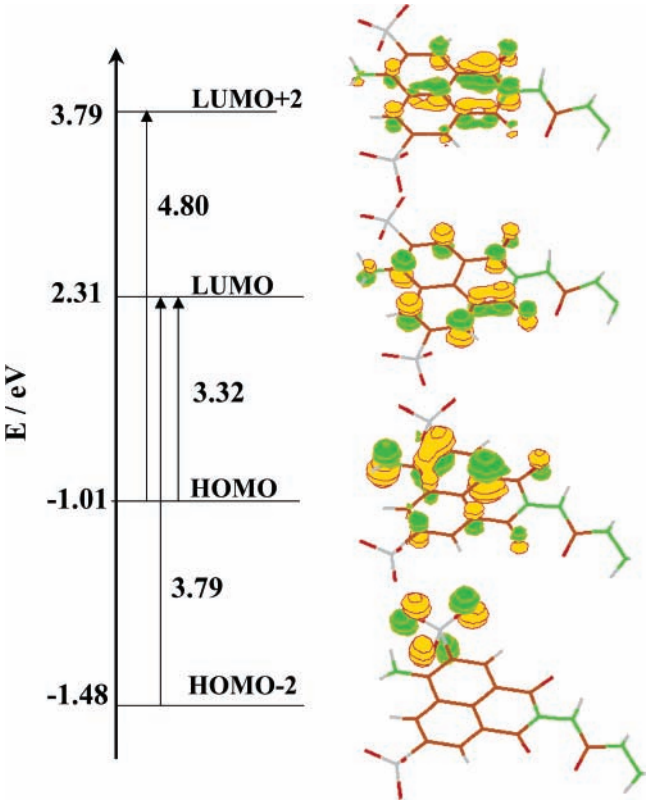

Figure 4. Kohn−Sham orbital contours involved in the key vertical excitations computed at the TD-DFT/B3LYP/6-31+G*//B3LYP/6-31G* level for the LY CH.

Fluorescence Experiments in Solvent Mixtures. Tertiary butanol is a viscous liquid, and its mixtures with water are often used in studies of viscosity dependence of excited-state processes. It is the preferred mixture in many cases due to the significant amount of changes in solvent structure present in the mixture. Besides, the viscosities of the mixture, at different compositions, are well characterized.[12a,b] A plot of log k_{NR} against the viscosities of the mixtures is found to be nonlinear, decreasing up to a viscosity of 4 mPa s and increasing slightly

TABLE 2: Important Vertical Excitations Computed at the TD-DFT/B3LYP/6-31+G*//B3LYP/6-31G* Level for the $[LY\ CH]^{2-}$

energy in (cm^{-1})	oscillator strength	$\psi_o - \psi_v$[a,b]	type of transition[c]
		Gas Phase	
22978	0.0004	HOMO − 1 → LUMO (0.70)	$\pi_{naph} \rightarrow \pi^*_{naph}$, C=O
24116	0.1877	HOMO → LUMO (0.64)	$\pi_{naph} \rightarrow \pi^*_{naph}$, C=O, imide
25925	0.0014	HOMO − 2[d] f LUMO (0.70)	$n_O \rightarrow \pi^*_{naph}$, C=O
		Condensed Phase (Water)[e]	
24337	0.1855	HOMO → LUMO (0.64)	$\pi_{naph} \rightarrow \pi^*_{naph}$, C=O
30197	0.0048	HOMO − 1 → LUMO (0.63)	$n_N \rightarrow \pi^*_{naph}$, C=O
31288	0.0005	HOMO − 2[d] → LUMO (0.65)	$n_{SO3} \rightarrow \pi^*_{naph}$, C=O

[a] Occupied and virtual orbitals. [b] Transition coefficient in parentheses. [c] π_{naph} represents a π-type MO located predominantly on the naphthyl unit. [d] Nonbonding orbital on sulfonyl oxygen. [e] Calculated using the IEFPCM//B3LYP/6-311G**//B3LYP/6-31G* level.

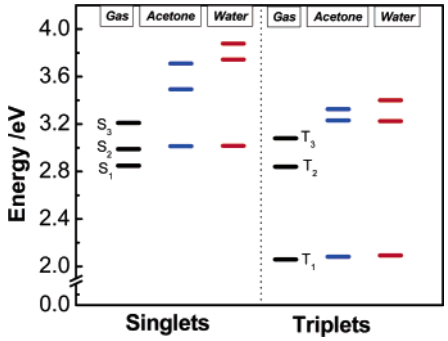

Figure 5. Energy level diagram depicting relative separation of various excited states for the LY CH in the gas phase (black), acetone (blue), and water (red) generated using the TD-DFT calculations.

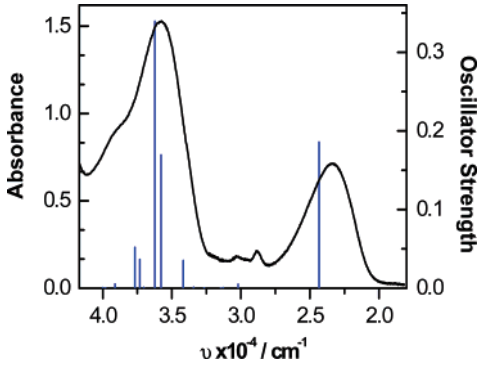

Figure 6. Comparison between computed vertical excitations (represented by blue vertical lines, proportional to the corresponding oscillator strengths) and the experimental absorption spectra for the LY CH in water.

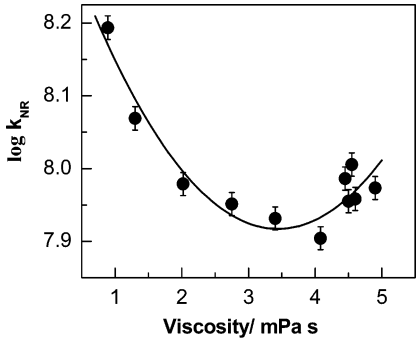

Figure 7. Variation of nonradiative rate (k_{NR}) of LY CH on the viscosity of water−^{t}butanol mixtures.

thereafter (Figure 7). The initial decrease is similar to that observed for intramolecular proton transfer in molecules such as hypocrellin A and B.[12c,d] The increase in k_{NR} at higher viscosities could be due to the interplay of empirical polarity and viscosity, as at high viscosities, the empirical polarity of

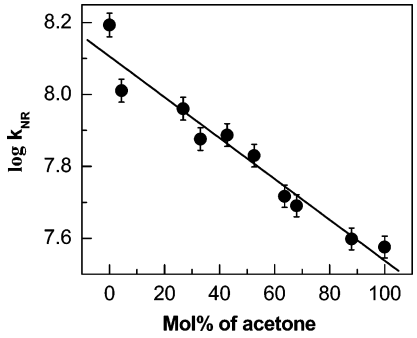

Figure 8. Variation of nonradiative rate (k_{NR}) of LY CH on the proticity: water−acetone mixtures.

the mixture is significantly lower than that of water. Thus, we observe a viscosity dependence which could indicate an excited-state process, most likely to be ESPT, associated with the motion of the carbohydrazine chain, similar to that observed in calphostin C.[4b] We have also measured the nonradiative rates in mixtures of acetone, an aprotic solvent, and water, a protic solvent. The variation of log k_{NR} with the mol fraction of acetone is linear, and there is jump in log k_{NR} at low mol fraction of water (Figure 8). Per se, this result would seem to indicate that proticity is not an important factor, but from the experiment on water−^{t}butanol mixtures, it is known that empirical polarity is also an important parameter. Thus, the observations in the acetone−water mixtures could be due to the interplay of empirical polarity and proticity with an effect of masking each other. It is useful to remember that the increase in k_{NR} with $E_T(30)$ is observed only in alcohols and water, which are protic solvents. Proticity of the solvent is an important factor in the determination of the photophysics of LY CH. However, this result does not rule out the possibility of an ESIPT process, as the two solvents differ significantly in empirical polarity, and this effect, convoluted with the change in proticity, can complicate the situation to a rather large extent.

Effect of Deuterated Solvents on Nonradiative Deactivation. The studies in the solvent mixtures do not conclusively establish or rule out the possibility of the ESPT process in LY CH. To obtain a clean picture, we measured the nonradiative rates in deuterated solvents. Whether an excited-state process such as solvent-mediated ESIPT would exhibit an isotope effect or not is predominantly governed by the molecular geometry. There are molecules that undergo ESPT but do not exhibit isotope effect.[4a,13a] This is generally explained by the consideration that the reaction coordinate is not the same as the proton-transfer coordinate. On the other hand, molecules such as 9-(2′-hydroxyphenyl)anthracene and *o*-aminoacetophenone exhibit a strong isotope effect.[13b,c] In this work, D_2O, MeOD, and EtOD have been used in order to examine the occurrence ESPT in LY CH. Emission spectra of LY CH in deuterated solvents show no shift in peak position relative to that of their parent ones, as

TABLE 3: Effect of Deuterated Solvents on Nonradiative Deactivation Rates of [LY CH]$^{2-}$

medium	$E_T(30)^a$	ϕ_f	$\langle\tau_f\rangle$ (ns)	$k_R \times 10^8$ (s^{-1})	$k_{NR} \times 10^8$ (s^{-1})
H_2O	63.1	0.21	5.04	0.42	1.57
D_2O	62.8	0.36	11.47	0.31	0.56
MeOH	55.4	0.55	9.50	0.58	0.47
MeOD		0.82	13.50	0.61	0.13
EtOH	51.9	0.62	10.07	0.62	0.38
EtOD		0.77	13.30	0.58	0.17

[a] Ref 11e.

shown in Figure 1a. However, the fluorescence quantum yields are significantly greater in the deuterated solvents (Table 3). Fluorescence lifetimes are also significantly increased as, for example, in water the lifetime is 5.06 ns while that in D_2O is 11.47 ns. Nonradiative rates of LY CH are considerably suppressed in deuterated solvents relative to that of their parent one (Table 3). This result clearly indicates that the ESPT is the governing parameter for nonradiative deactivation of LY CH in the polar protic region.

4. Conclusion

The solvent variation as well as the ab initio quantum chemical calculations indicate that the principal nonradiative channel is likely to be ISC in nonalcoholic solvents and some other excited-state process in alcohols and water. The B3LYP/6-31G* optimized structure reveals an intramolecular N−H···O hydrogen bonding indicating that a possible intramolecular proton transfer in the excited state may be possible from the point of view of the molecular geometry. A marked dependence of the nonradiative rate on the viscosity is observed, indicating the coupling of the excited-state process with conformational changes in the molecule. This may be rationalized by either an intramolecular proton transfer involving the carbohydrazine chain or a TICT model, both of which involve the relative motion of different segments of the molecule with respect to each other. However, TICT usually leads to either a highly Stokes-shifted emission band or a nonradiative state.[14] In the present case, the Stokes shift in water is not remarkably different from that in the lowest polarity solvent used and the decrease in fluorescence quantum yield is no more than a factor of 3. Thus, a TICT model does not seem to be applicable. The marked isotope effects in the protic solvents provide a conclusive evidence of a solvent-mediated ESPT. However, the dependence of the nonradiative rate on the viscosity of the medium indicates that the proton transfer is intramolecular, as an intermolecular proton transfer with the solvent would not be slowed in solvents of higher viscosity. These results serve to explain our earlier observation that the nonradiative rate decreases upon incorporation in CTAB micelle, in terms of hindrance provided to the solvent-mediated ESIPT, mainly due to sequestering of the fluorophore from the water molecules by the micelles and further, due to the increased viscosity in the micellar region.

To further substantiate the findings of the present work, the presence of photolabile protons needs to be tested in future. Experiments in the femtosecond time scale as well as synthetic modification of the probe such as replacement of hydrogen atom attached to N3 of LY CH by a methyl group might be useful to further elucidate the nature of the excited-state dynamics. Moreover, the understanding generated about the basic photophysics of LY CH in the present study can be utilized in exploration of its potential implications in photobiology.[15]

Acknowledgment. This work is supported by CSIR Research Grant No. 01 (1851)/03/EMR-II. D.P. thanks CSIR for a Junior Research Fellowship. IIT Bombay computer center is acknowledged for computing facilities.

Supporting Information Available: The B3LYP/6-31G* optimized geometry in the form of Cartesian coordinates, total electronic energy, vertical excitations in different polar solvents, etc. This material is available free of charge via the Internet at http://pubs.acs.org.

References and Notes

(1) (a) Stewart, W. W. *Nature* **1981**, *292*, 17. (b) Stewart, W. W. *J. Am. Chem. Soc.* **1981**, *103*, 7615. (c) Lee, J. A.; Fortes, P. A. G. *Biochemistry* **1986**, *25*, 8133. (d) Cunningham, K. M.; McCarty, R. E. *Biochemistry* **2000**, *39*, 4391. (e) Mayr, T.; Werner, T. *Analyst* **2002**, *127*, 248.

(2) (a) Peracchia, C. *Nature* **1981**, *290*, 597. (b) Sommer, A.; Georges, R.; Kostner, G. M.; Paltauf, F.; Hermetter, A. *Biochemistry* **1991**, *30*, 11245. (c) Rocha, M.; Sur, M. *Proc. Natl. Acad. Sci. U.S.A.* **1995**, *92*, 8026. (d) Suh, B. C.; Song, S. K.; Kim, Y. K.; Kim, K. T. *J. Biol. Chem.* **1996**, *271*, 32753.

(3) (a) Saha, S.; Samta, A. *J. Phys. Chem. A* **2002**, *106*, 4763. (b) Mishra, P. P.; Koner, A. L.; Datta, A. *Chem. Phys. Lett.* **2004**, *400*, 128. (c) Fürstenberg, A.; Vauthey, E. *Photochem. Photobiol. Sci.* **2005**, *4*, 260.

(4) (a) Petrich, J. W. *Int. Rev. Phys. Chem.* **2000**, *19*, 479. (b) Datta, A.; Bandyopadhyay, P.; Wen, J.; Petrich, J. W.; Gordon, M. S. *J. Phys. Chem. A* **2000**, *105*, 1057. (c) Cave, R. J.; Castner, E. W., Jr. *J. Phys. Chem. A* **2002**, *106*, 12117. (d) Banuelos Prieto, J.; López Arbeloa, F.; Martínez Martínez, V.; Arebola López, T.; López Arbeloa, I. *Phys. Chem. Chem. Phys.* **2004**, *6*, 4247.

(5) (a) O'Neil, M. P.; Wasielewski, M. R.; Khaled, M. M.; Kispert, L. D. *J. Chem. Phys.* **1991**, *95*, 7212. (b) Rechthaler, K.; Köhler, G. *Chem. Phys.* **1994**, *189*, 99. (c) Nad, S.; Pal, H. *J. Phys. Chem. A* **2001**, *105*, 1097. (d) López Arbeloa, F.; Banuelos Prieto, J.; Martínez Martínez, V.; Arebola López, T.; López Arbeloa, I. *ChemPhysChem* **2004**, *5*, 1762.

(6) (a) Das, K; Sarkar, N.; Ghosh, A. K.; Majumdar, D.; Nath, D. N.; Bhattacharyya, K. *J. Phys. Chem.* **1994**, *98*, 9126. (b) Sarkar, N.; Das, K.; Nath, D. N.; Bhattacharyya, K. *Langmuir*, **1995**, *10*, 326. (c) Pal, H.; Nad, S.; Kumbhakar, M. *J. Chem. Phys.* **2003**, *119*, 443.

(7) (a) Il'ichev, Yu. V.; Kühnle, W.; Zachariasse, K. A. *J. Phys. Chem. A* **1998**, *102*, 670. (b) Smirnov, A. V.; Das, K.; English, D. S.; Wan, Z.; Kraus, G. A.; Petrich, J. W. *J. Phys. Chem. A* **1999**, *103*, 7949. (c) Dobkowski, J.; Rettig, W.; Waluk, J. *Phys. Chem. Chem. Phys.* **2002**, *4*, 4334.

(8) (a) Klymchenko, A. S.; Demchenko, A. P.; *J. Am. Chem. Soc.* **2002**, *124*, 12372. (b) Gromov, E. V.; Burghardt, I.; Koppel, H.; Cederbaum, L. S. *J. Phys. Chem. A* **2005**, *109*, 4623.

(9) (a) Seybold, P. G.; Gouterman, M. *J. Mol. Spectrosc.* **1969**, *31*, 1. (b) Mukherjee, T. K.; Mishra, P. P.; Datta, A. *Chem. Phys. Lett.* **2005**, *407*, 119.

(10) (a) Becke, A. D. *J. Chem. Phys.* **1993**, *98*, 5648. (b) Becke, A. D. *J. Chem. Phys.* **1993**, *98*, 1372. (c) Frisch, M. J.; Trucks, G. W.; Schlegel, H. B.; Scuseria, G. E.; Robb, M. A.; Cheeseman, J. R.; Zakrzewski, V. G.; Montgomery, J. A., Jr.; Stratmann, R. E.; Burant, J. C.; Dapprich, S.; Millam, J. M.; Daniels, A. D.; Kudin, K. N.; Strain, M. C.; Farkas, O.; Tomasi, J.; Barone, V.; Cossi, M.; Cammi, R.; Mennucci, B.; Pomelli, C.; Adamo, C.; Clifford, S.; Ochterski, J.; Petersson, G. A.; Ayala, P. Y.; Cui, Q.; Morokuma, K.; Malick, D. K.; Rabuck, A. D.; Raghavachari, K.; Foresman, J. B.; Cioslowski, J.; Ortiz, J. V.; Stefanov, B. B.; Liu, G.; Liashenko, A.; Piskorz, P.; Komaromi, I.; Gomperts, R.; Martin, R. L.; Fox, D. J.; Keith, T.; Al-Laham, M. A.; Peng, C. Y.; Nanayakkara, A.; Gonzalez, C.; Challacombe, M.; Gill, P. M. W.; Johnson, B. G.; Chen, W.; Wong, M. W.; Andres, J. L.; Head-Gordon, M.; Replogle, E. S.; Pople, J. A. *Gaussian 98*; Gaussian, Inc.: Pittsburgh, PA, 1998. (d) Wiberg, K. G.; Stratmann, R. E.; Frisch, M. J. *J. Chem. Phys.* **1998**, *297*, 60. (e) Schaftenaar, G.; Noordik, J. H. *J. Comput.-Aided Mol. Des.* **2000**, *14*, 123. (f) Tomasi, J.; Persico, M. *Chem. Rev.* **1994**, *94*, 2027. (g) Mennucci, B.; Cances, E.; Tomasi, J. *J. Phys. Chem. B* **1997**, *101*, 10506. (h) See the Supporting Information.

(11) (a) Seliskar, C. J.; Brand, L. *J. Am. Chem. Soc.* **1971**, *93*, 5414. (b) Rettig, W.; Majenz, W.; Herter, R.; Létard; J.-F.; Lapouyade, R. *Pure Appl. Chem.* **1993**, *65*, 1699. (c) Eisenthal, K. B. *Chem. Rev.* **1996**, *96*, 1343. (d) Herodes, K.; Koppel, J.; Reichardt, C.; Koppel, I. A. *J. Phys. Org. Chem.* **2003**, *16*, 626. (e) Reichardt, C. *Pure Appl. Chem.* **2004**, *76*, 1903.

(12) (a) Senanayake, P. C.; Freeman, G. R. *J. Phys. Chem.* **1987**, *91*, 2123. (b) Dutt, G. B.; Doraiswamy, S.; Periasamy, N. *J. Chem. Phys.* **1991**, *94*, 5360. (c) Das, K.; English, D. S.; Petrich, J. W. *J. Am. Chem. Soc.* **1997**, *119*, 2763. (d) Datta, A.; Smirnov, A. V.; Wen, J.; Chumanov, G.; Petrich, J. W. *Photochem. Photobiol.* **2000**, *71*, 166.

(13) (a) Frey, W.; Laermer, F.; EIsaesser, T. *J. Phys. Chem.* **1991**, *95*, 10391. (b) Mitchel, F.; Matthew, L.; Lawrence, H.; Peter, W. *J. Am. Chem. Soc.* **2004**, *126*, 7890. (c) Yoshihara, T.; Shimada, H.; Shizuka, H.; Tobita, S. *Phys. Chem. Chem. Phys.* **2001**, *3*, 4972.

(14) Grabowski, Z. R.; Rotkiewicz, K.; Rettig, W. *Chem. Rev.* **2003**, *103*, 3899.

(15) (a) Brana, M. F.; Dominguez, G.; Saez, B.; Romerdahl, C.; Robinson, S.; Barlozzari, T. *Eur. J. Med. Chem.* **2002**, *37*, 541−551. (b) Brana, M. F.; Castellano, J. M.; Moran, M.; Perez de Vega, M. J.; Perron, D.; Conlon, D.; Bousquet, P. F.; Romerdahl, C. A.; Robinson, S. P. *Anti-Cancer Drug Des.* **1996**, 297−309. (c) Matsugo, S.; Kawanishi, S.; Yamamoto, K.; Sugiyama, H.; Matsura, T.; Saito, I. *Angew. Chem., Int. Ed. Engl.* **1991**, *30*, 1351−1353.